© 2014. Published by The Company of Biologists Ltd | Development (2014) 141, 3697-3708 doi:10.1242/dev.110833

RESEARCH ARTICLE

# Multiple roles for HOXA3 in regulating thymus and parathyroid differentiation and morphogenesis in mouse

**Jena L. Chojnowski[1], Kyoko Masuda[1,*], Heidi A. Trau[1,‡], Kirk Thomas[2], Mario Capecchi[3] and Nancy R. Manley[1,§]**

## ABSTRACT

*Hoxa3* was the first Hox gene to be mutated by gene targeting in mice and is required for the development of multiple endoderm and neural crest cell (NCC)-derived structures in the pharyngeal region. Previous studies have shown that the *Hoxa3* null mutant lacks third pharyngeal pouch derivatives, the thymus and parathyroids by E18.5, and organ-specific markers are absent or downregulated during initial organogenesis. Our current analysis of the *Hoxa3* null mutant shows that organ-specific domains did undergo initial patterning, but the location and timing of key regional markers within the pouch, including *Tbx1*, *Bmp4* and *Fgf8*, were altered. Expression of the parathyroid marker *Gcm2* was initiated but was quickly downregulated and differentiation failed; by contrast, thymus markers were delayed but achieved normal levels, concurrent with complete loss through apoptosis. To determine the cell type-specific roles of *Hoxa3* in third pharyngeal pouch development, we analyzed tissue-specific mutants using endoderm and/or NCC-specific Cre drivers. Simultaneous deletion with both drivers resulted in athymia at E18.5, similar to the null. By contrast, the individual tissue-specific *Hoxa3* deletions resulted in small, ectopic thymi, although each had a unique phenotype. *Hoxa3* was primarily required in NCCs for morphogenesis. In endoderm, *Hoxa3* temporally regulated initiation of the thymus program and was required in a cell-autonomous manner for parathyroid differentiation. Furthermore, *Hoxa3* was required for survival of third pharyngeal pouch-derived organs, but expression in either tissue was sufficient for this function. These data show that *Hoxa3* has multiple complex and tissue-specific functions during patterning, differentiation and morphogenesis of the thymus and parathyroids.

**KEY WORDS: Hoxa3, Thymus, Parathyroid, Mouse**

## INTRODUCTION

HOX proteins are a highly conserved family of transcription factors that play essential roles in defining axial identity during metazoan development. Mouse knockout studies have shown that mutations in individual Hox genes affect multiple tissues within the region associated with its anterior boundary of expression, suggesting that vertebrate Hox genes control regional identity (Mallo et al., 2010). However, although many Hox gene null phenotypes in mice have been described, little is known about how HOX proteins regulate tissue-specific pathways.

*Hoxa3* was the first Hox gene to be mutated in mice by homologous recombination, and the null phenotype has been well characterized (Chisaka and Capecchi, 1991; Manley and Capecchi, 1995, 1998; Su et al., 2001; Kameda et al., 2002, 2003, 2004; Gaufo et al., 2003). *Hoxa3* has an anterior expression limit at the third pharyngeal arch and is expressed in all cell populations in the pharyngeal region, including endoderm, ectoderm, mesoderm and neural crest cells (NCCs) (Gaunt, 1987, 1988; Chisaka and Capecchi, 1991; Manley and Capecchi, 1995). It has been implicated in patterning, cell migration, proliferation, apoptosis and differentiation. $Hoxa3^{null}$ mice have normal initial formation of the pharyngeal arches and pouches, but severe defects in pharyngeal development, including athymia and aparathyroidism, as well as other organ, skeletal and nerve defects. *Hoxa3* is the only *Hox3* paralog that is required for thymus and parathyroid initial organogenesis, as mice with only a single wild-type *Hoxa3* allele ($Hoxa3^{+/-}Hoxb3^{-/-}Hoxd3^{-/-}$) have both organs, albeit ectopically located (Manley and Capecchi, 1998).

The thymus and parathyroids are derived from the third pharyngeal pouch and are identifiable as separate organ domains within the same primordium by the expression patterns of organ-specific genes beginning at embryonic day 10.5 (E10.5). *Gcm2* (*glial cells missing 2*) is a parathyroid marker that is necessary for differentiation and survival (Gunther et al., 2000; Gordon et al., 2001; Liu et al., 2007). At E11.0, *Foxn1* (*Forkhead box N1*) expression marks the thymus domain and is necessary for thymic epithelial cell (TEC) proliferation and differentiation (Nehls et al., 1994, 1996; Manley and Condie, 2010). Previously, we have shown that in the $Hoxa3^{null}$ mouse, *Gcm2* is reduced at E10.5 and *Foxn1* is lacking at E11.5 (Chen et al., 2010); other parathyroid differentiation markers are also undetectable at E12.0 (Kameda et al., 2004). As Hox genes are classically considered to specify positional identity, these molecular data together with the perinatal phenotype suggest that HOXA3 acts to specify third pharyngeal pouch identity and that, in its absence, organ specification fails (Manley and Condie, 2010).

Proper specification of thymus and parathyroid fate and subsequent organ development require interactions between third pharyngeal pouch endoderm and surrounding NC-derived mesenchyme, both of which express *Hoxa3* (Manley and Condie, 2010; Gordon and Manley, 2011; Manley et al., 2011). Several signaling pathways have been implicated in third pharyngeal pouch patterning and organ development. *Fgf8* and *Bmp4* are expressed in the presumptive thymus domain before *Foxn1* expression, and *Bmp4* is also expressed in the surrounding NC-derived mesenchyme (Ohuchi et al., 2000; Revest et al., 2001; Frank et al., 2002; Patel et al., 2006; Gardiner et al., 2012). BMP signaling has been

[1]Department of Genetics, Paul D. Coverdell Center, 500 DW Brooks Drive, University of Georgia, Athens, GA 30602, USA. [2]Division of Hematology and Program in Molecular Medicine, University of Utah School of Medicine, Salt Lake City, UT 84132, USA. [3]Department of Human Genetics, Howard Hughes Medical Institute, University of Utah School of Medicine, Salt Lake City, UT 84132, USA. *Present address: The Institute of Frontier Medical Sciences, Kyoto University, 53 Shogoin-Kawahara-cho, Sakyo-ku, Kyoto-shi, Kyoto 606-8397, Japan. ‡Present address: Department of Physiological Sciences, Eastern Virginia Medical School, 700 Olney Road, Lewis Hall, Norfolk, VA 23507, USA.

§Author for correspondence (nmanley@uga.edu)

**Received 31 March 2014; Accepted 30 July 2014**

Development (2014) 141, 3697-3708 doi:10.1242/dev.110833

implicated in regulating *Foxn1* expression in mice, chick and zebrafish (Ohnemus et al., 2002; Bleul and Boehm, 2005; Wang et al., 2006; Soza-Ried et al., 2008; Gordon et al., 2010). Recent data obtained from chick suggests that sequential BMP-FGF signaling is sufficient to establish thymus fate (Neves et al., 2012). By contrast, SHH signaling promotes parathyroid fate and is a negative regulator of thymus fate. In its absence, embryos lack *Gcm2*, downregulate *Tbx1* and expand *Bmp4* and *Foxn1* expression throughout the developing primordium (Moore-Scott and Manley, 2005; Grevellec et al., 2011). We have previously proposed that BMP4 and SHH act in opposition to pattern the thymus and parathyroid domains (Gordon and Manley, 2011). Linking these signaling pathways to HOXA3 will begin to shape the regulatory network that specifies the third pharyngeal pouch regional identity and differentiation.

Here, we have evaluated cell type-specific functions of HOXA3 in thymus and parathyroid development by generating tissue-specific deletions in endoderm and/or NCCs and re-evaluated the null mutant to better understand HOXA3 function. To our surprise, parathyroid and thymus differentiation was initiated in *Hoxa3*$^{-/-}$ mutants, albeit with patterning and timing defects. Consistent with the published phenotype, both organs ultimately failed to develop, although the role of HOXA3 was different in each organ. Furthermore, each tissue-specific deletion resulted in small, ectopic thymi and parathyroids by E18.5, although each cell type-specific mutant had a unique phenotype that was distinct from the null. Therefore, *Hoxa3* expression in either tissue is sufficient for thymus and parathyroid organogenesis and has distinct roles in each tissue. The combined results from the *Hoxa3* tissue-specific deletions and the null allele showed that HOXA3 is required for *Gcm2* upregulation and parathyroid survival, but has two distinct roles in thymus fate – an endoderm-intrinsic temporal role in potentiating the thymus program, and a separate, redundant function in both endoderm and NCCs to promote thymus survival. Finally, although HOXA3 regulates early organ morphogenesis, it is dispensable for later differentiation or survival.

## RESULTS

### Temporal and spatial expression of *Hoxa3* during early thymus-parathyroid development

We first performed a detailed analysis of the spatial and temporal *Hoxa3* expression pattern in the third pharyngeal pouch and developing organ primordia from E10.5 to E13.5, which encompass patterning and initial organogenesis. At E10.5, *Hoxa3* was expressed strongly and at similar levels in the third pharyngeal pouch endoderm and surrounding NCCs (Fig. 1A). At E11.0-E11.5, *Hoxa3* expression within the primordium decreased relative to that in the surrounding NCCs, where expression remained high (Fig. 1B,C). Expression in NCCs began to decline at E12.0 (Fig. 1D). By E12.5, *Hoxa3* expression in both tissues was low and, by E13.5, was undetectable using this assay (Fig. 1E,F), although it was detected in total thymic stroma at E15.5 by using reverse transcription (RT)-PCR (Su et al., 2001).

HOXA3 protein was detected to different extents within the E10.5 third pharyngeal pouch by using immunohistochemistry (IHC), with higher levels in the prospective dorsal-anterior parathyroid and ventral-posterior thymus domains (Gordon et al., 2001) and lower levels in the remaining posterior-dorsal domain (Fig. 1G,H). By contrast, protein levels in surrounding NCCs were more uniform (Fig. 1G).

Taken together, these data suggested that HOXA3 in both cell types might affect early third pharyngeal pouch development, with the influence in the endoderm restricted primarily to early patterning, whereas HOXA3 in the surrounding NCCs might also act in later morphogenetic events.

### HOXA3 modulates, but is not required for, thymus- and parathyroid-specific gene expression

Our expression analysis suggested that there is the potential for both overlapping and distinct functions of HOXA3 in the endoderm and NCCs during third pharyngeal pouch development. To provide a clear baseline of comparison for tissue-specific deletions, we characterized organ-specific patterning in the *Hoxa3*$^{-/-}$ mutant at the initial stages of third pharyngeal pouch organogenesis. The

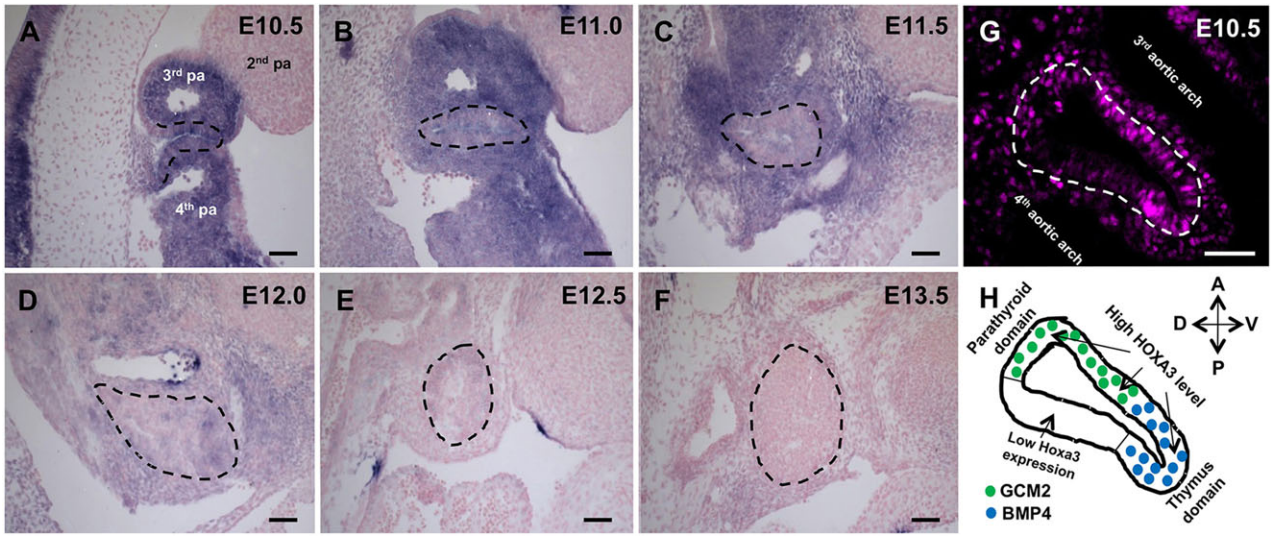


**Fig. 1. *Hoxa3* is differentially expressed in the endoderm and NCCs between E10.5 and E13.5.** (A-F) Sagittal sections of E10.5-E13.5 wild-type embryos that had been subjected to ISH with a *Hoxa3* riboprobe (blue). Staining for all sections was performed together and for an equal length of time. (G) HOXA3 immunofluorescence (magenta) in a wild-type embryo (*n*=8) at E10.5. (H) Diagram indicating the E10.5 third pharyngeal pouch domains with expression of GCM2 and BMP4 (Patel et al., 2006) and the corresponding levels of HOXA3. The third pharyngeal pouch is outlined in all panels. A, anterior; D, dorsal; P, posterior; pa, pharyngeal arch; V, ventral. Scale bars: 40 µm.

Development (2014) 141, 3697-3708 doi:10.1242/dev.110833

TEC-specific marker *Foxn1* is normally detected at approximately E11.25 but was absent in the hypoplastic primordia in *Hoxa3*$^{-/-}$ mutants at E11.5 (Fig. 2A,B). However, *Foxn1* expression was detected in the null at low levels by E12, about a day later than the control, and attained a normal expression pattern and levels by E12.5 (Fig. 2C-F). These small thymi also expressed the FOXN1-independent thymus marker, *Il7* (Zamisch et al., 2005) at higher levels than controls (Fig. 2G,J), indicating that they were differentiating as thymus. We also assessed expression of *Foxg1*, which encodes a transcription factor that is normally present in the prospective thymus domain at E10.5 before and independently of *Foxn1* expression, and is maintained throughout thymus development (Wei and Condie, 2011). *Foxg1* is also expressed in an unspecified dorsal-posterior domain at E10.5 (Wei and Condie, 2011). In the *Hoxa3*$^{-/-}$ mutant at E10.5, *Foxg1* was expressed in the dorsal-posterior domain but was absent from the thymus domain (Fig. 2I,J). By E11.5, *Foxg1* was expressed throughout most of the primordium (Fig. 2K,L). This *Foxg1* expression delay in the thymus domain is similar to that seen for *Foxn1* expression, suggesting that thymus fate specification is generally delayed in the *Hoxa3*$^{-/-}$ mutants.

The parathyroid marker *Gcm2* is usually expressed in a dorsal-anterior domain of the third pharyngeal pouch at E10.5 (Gordon et al., 2001). As we have previously reported (Chen et al., 2010), *Hoxa3*$^{-/-}$ embryos had dramatically reduced but correctly localized expression of *Gcm2* at E10.5 (Fig. 2M,N). TBX1 is a transcription factor that is also restricted to the parathyroid domain at E10.5 and is independent of *Gcm2* (Garg et al., 2001; Liu et al., 2007; Grevellec et al., 2011). The *Tbx1* expression domain was present but reduced in *Hoxa3*$^{-/-}$ mutants (Fig. 2O,P). By E11.5, *Gcm2* expression was undetectable (Fig. 2Q-T). A small group of *Gcm2 Foxn1* double-negative cells that was attached to the thymus persisted until E12.5 (Fig. 2D,F,R,T), but was undetectable by E13.0 (Fig. 3H,I). These results are consistent with previous reports that show the absence of other parathyroid differentiation markers at E11.5 (Kameda et al., 2004) and the loss of prospective parathyroid cells through apoptosis at E12.5 in *Gcm2*$^{-/-}$ mutants (Liu et al., 2007).

ΔNp63 is reported to mark thymic epithelial precursor cells (Senoo et al., 2007), although its expression before E12.0 in the third pharyngeal pouch has not been described. At E10.5, ΔNp63 protein levels were variable and low in the third pharyngeal pouch in both controls and mutants (Fig. 3A,B). By E11.5, ΔNp63 was only present in GCM2-negative cells, marking the thymus domain (Fig. 3C). In the E11.5 *Hoxa3*$^{-/-}$ mutant, ΔNp63 was present throughout the primordium (Fig. 3D). This result and the loss of GCM2 suggest that in the null mutant, these dorsal cells initiate, but fail to establish, parathyroid fate by E11.5. As these cells also did not acquire a *Foxn1*-positive thymic fate (Fig. 2E,F), the absence of GCM2 results in their death by apoptosis around E12.5.

SHH signaling is required for *Gcm2* expression and parathyroid fate specification and also regulates *Tbx1* (Garg et al., 2001; Moore-Scott and Manley, 2005; Grevellec et al., 2011). HOXA3 does not appear to act downstream of SHH, as *Hoxa3* expression is unaffected in *Shh*$^{-/-}$ mutants (Moore-Scott and Manley, 2005).

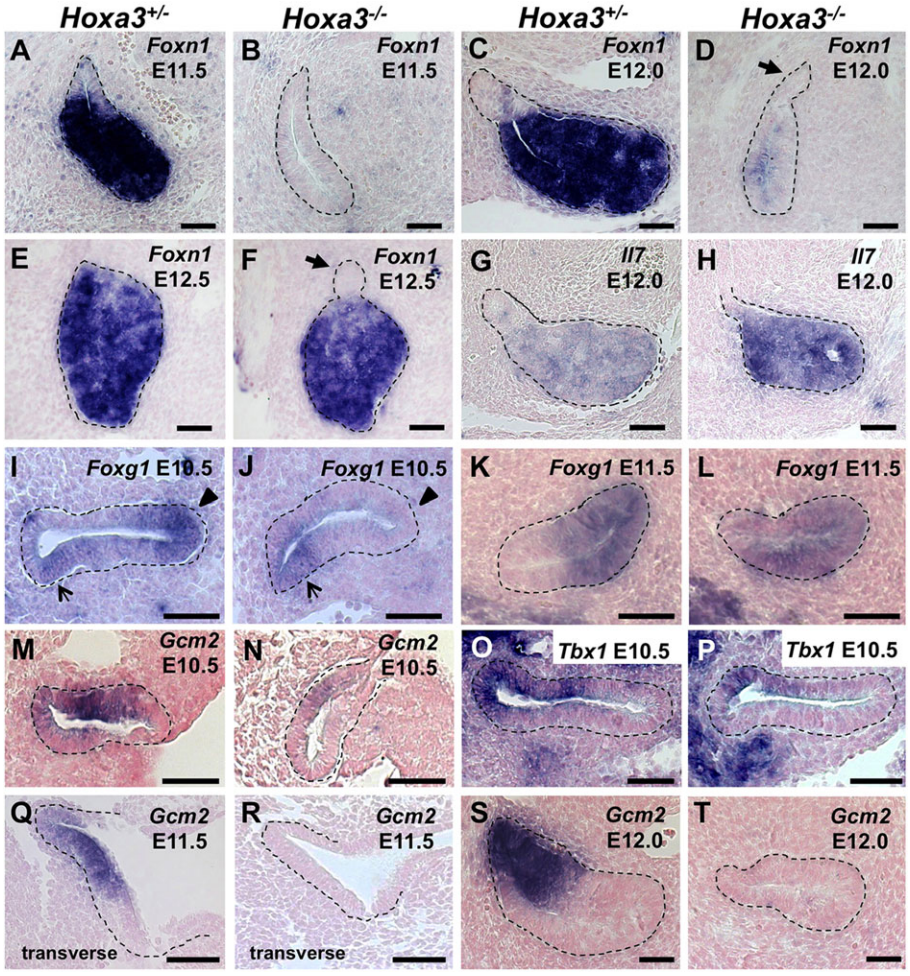


**Fig. 2. *Foxn1*, *Il7*, *Foxg1*, *Gcm2*, and *Tbx1* are mis-expressed in *Hoxa3*$^{-/-}$ mutants.** ISH of paraffin sections from *Hoxa3*$^{+/-}$ and *Hoxa3*$^{-/-}$ embryos. (A-F) Sagittal sections at E11.5 (*n*=3), E12.0 (*n*=2) and E12.5 (*n*=1) were stained with a *Foxn1* riboprobe. Arrows indicate a group of *Foxn1*-negative cells attached to the thymus at E12.0 and E12.5. (G,H) Sagittal sections at E12.0 were stained with an *Il7* riboprobe (*n*=2). (I-L) Sagittal sections at E10.5 (*n*=2) and E11.5 (*n*=2) were stained with a *Foxg1* riboprobe. *Foxg1* expression in the *Hoxa3*$^{-/-}$ is absent in the thymus domain (arrowheads) but present in the dorsal-posterior domain at E10.5 (arrows). Sagittal sections at E10.5 (*n*=4) (M,N), transverse sections at E11.5 (*n*=3) (Q,R) and sagittal sections at E12.0 (*n*=2) (S,T) were stained with a *Gcm2* riboprobe. (O,P) Sagittal sections at E10.5 (*n*=2) were stained with a *Tbx1* riboprobe. In all sections, anterior is towards the top of the image, and the same side is presented per stage and gene. The third pharyngeal pouch is outlined in all panels. Scale bars: 40 μm.

Development (2014) 141, 3697-3708 doi:10.1242/dev.110833

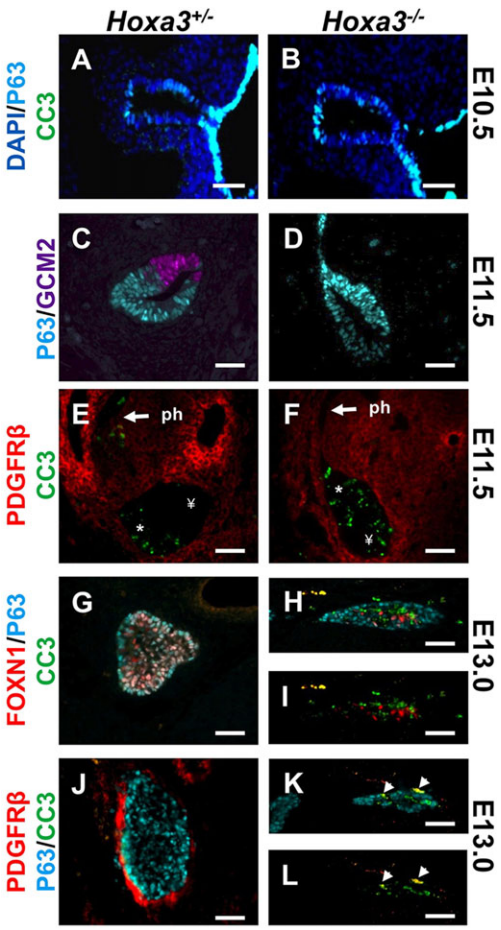


**Fig. 3. The parathyroid and thymus are lost in *Hoxa3*$^{-/-}$ mutants.** Immunostaining of sagittal E10.5 (*n*=2) (A,B), E11.5 (*n*=3 each set) (C-F) and transverse E13.0 (*n*=3 each set) (G-L) sections of the *Hoxa3*$^{+/-}$ and *Hoxa3*$^{-/-}$ thymus with antibodies against cleaved caspase-3 (CC3), p63, GCM2, PDGFRβ and FOXN1. DAPI stains nuclei. *, the region within the primordium that normally undergoes apoptosis during separation from the pharynx. ¥, the posterior-dorsal region that does not normally undergo apoptosis. Arrows indicate the thymus-pharynx (ph) attachment domain that normally undergoes apoptosis. Arrowheads indicate co-labeling of PDGFR and CC3. Scale bars: 40 µm.

To further investigate this potential relationship, we assessed *Ptch1* expression in *Hoxa3*$^{-/-}$ mutants. SHH signaling was unaffected in *Hoxa3*$^{-/-}$ mutants at E10.5, as indicated by *Ptch1*$^{lacZ}$ expression (supplementary material Fig. S3A,B). These data suggest that HOXA3 and SHH signaling act in distinct pathways to affect parathyroid fate specification and differentiation.

These data show that the expression of regionally restricted markers is disrupted in the *Hoxa3*$^{-/-}$ mutants, but not in a uniform way. As a result, although the expression of both *Gcm2* and *Foxn1* is initially delayed and/or reduced relative to wild type, these markers are ultimately affected in opposite ways (*Foxn1* expression is delayed and then normal, *Gcm2* expression is low and then absent). Despite these distinct phenotypes, both organs are absent at later stages (Chisaka and Capecchi, 1991; Manley and Capecchi, 1995).

### *Hoxa3* is necessary for thymus and parathyroid survival

Despite the initiation of thymus differentiation in *Hoxa3*$^{-/-}$ mutants, the primordia were absent at E13.5. Although at E10.5 both mutant and control third pharyngeal pouch cells were negative for the cell death marker cleaved caspase-3 (CC3) (Fig. 3A,B), between E11.5 and E13.5, substantial apoptosis was present in the mutant primordia (Fig. 3E-L). At E11.5 in control embryos, apoptotic cells were restricted to the region where the thymus domain was attached to the pharynx (Fig. 3E); this is the normal mechanism for thymus-pharynx separation (Gordon et al., 2004; Gardiner et al., 2012). By contrast, *Hoxa3*$^{-/-}$ mutants had CC3-positive cells throughout the primordium, but not in the pharynx (Fig. 3F). This phenotype continued at E13.0, with numerous apoptotic cells throughout the mutant primordium (Fig. 3G). Interestingly, CC3-positive epithelial cells did not co-label with either FOXN1 or ΔNp63 (Fig. 3G-I). However, we could not distinguish whether downregulation of these markers induced apoptosis, or that these markers were degraded rapidly during apoptosis and thus undetectable. A subset of CC3-positive cells on the perimeter of the E13.0 (but not E11.5) primordium were co-labeled with PDGFRβ, an NCC marker (Fig. 3E,F,J-L). Because *Hoxa3* is normally downregulated in NCCs by E12.5 (Fig. 1E,F), the timing of mesenchymal cell death suggests that the NCC-derived capsule undergoes apoptosis secondarily in response to primordium collapse.

### *Hoxa3* expression in either endoderm or neural crest is sufficient for organ development

Both our expression data and other published studies have suggested that HOXA3 in both NCCs and the endoderm influences early third pharyngeal pouch patterning and thymus and parathyroid organogenesis (Manley et al., 2011). To determine the tissue-specific roles of HOXA3, we deleted *Hoxa3* from NCCs and/or endoderm using a conditional allele (supplementary material Fig. S1) and the *Wnt1Cre* (Danielian et al., 1998) and/or *Foxa2*$^{CreERT2}$ (Park et al., 2008) strains. *Wnt1Cre* efficiently deleted *Hoxa3* in NCCs surrounding the third pharyngeal pouch (Fig. 4B,E). The tamoxifen-inducible *Foxa2*$^{CreERT2}$ allele caused endoderm-specific deletion throughout the third pharyngeal pouch, although a few cells had failed to delete *Hoxa3* by E10.5 (Fig. 4C,F,G; supplementary material Fig. S2A,B). This slight inefficiency led to low-level mosaic *Hoxa3* expression in the third pharyngeal pouch, allowing us to address the cell-autonomous role of *Hoxa3* in early organogenesis.

In contrast to the *Hoxa3*$^{-/-}$ mutant, both individual tissue-specific deletions resulted in small ectopic thymi and parathyroids (Fig. 5A-D,F-I), indicating that expression of *Hoxa3* in either cell type was sufficient for their organogenesis. To confirm that these are the only two cell types necessary for thymus and parathyroid development, we simultaneously deleted *Hoxa3* using both tissue-specific Cre strains. These mutants had a complete loss of the thymus and parathyroids at E18.5, similar to the previously published *Hoxa3*$^{null}$ (Fig. 5E,J). This result also indicated that the low level of mosaicism in the endoderm-specific mutants was unlikely to be the reason for the formation of the thymus in this model.

### Endodermal *Hoxa3* temporally regulates *Foxn1* expression

After *Hoxa3* endoderm-specific deletion, low FOXN1 levels were present at E12.0 in scattered cells throughout the ventral domain, similar to the timing of initial *Foxn1* mRNA expression in the null mutant (Fig. 6D,I; compare with Fig. 2A,B). A few individual cells were FOXN1 positive by late E11.25, around 10-14 h later than in the control thymus domain, but earlier than in the null mutant (Fig. 6A-C,F-H). These cells might represent HOXA3-expressing cells that are present after inefficient endoderm deletion (Fig. 4F; supplementary material Fig. S2B). Although the endoderm-specific mutant thymus was ~20% the size of the control thymus at E17.5 (Fig. 6O), it had normal

Development (2014) 141, 3697-3708 doi:10.1242/dev.110833

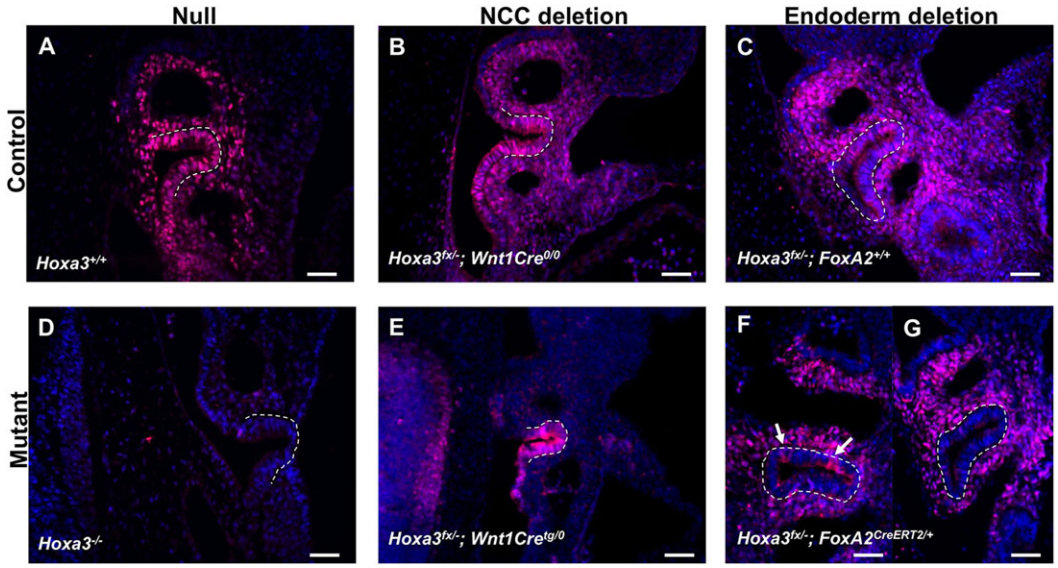


**Fig. 4. Deletion efficiency of *Hoxa3* in the null and after *Wnt1Cre* or *Foxa2*$^{CreERT2}$-mediated deletion.** Immunofluorescence for HOXA3 in the pharyngeal region of E10.5 sagittal sections in *Hoxa3*$^{+/+}$ (*n*=3) and *Hoxa3*$^{-/-}$ (*n*=3) embryos (A,D), in control (*Hoxa3*$^{fx/-}$;*Wnt1Cre*$^{0/0}$) and NCC deletion (*Hoxa3*$^{fx/-}$;*Wnt1Cre*$^{tg/0}$) embryos (*n*=2) (B,E), and in control (*Hoxa3*$^{fx/-}$;*Foxa2*$^{+/+}$) and endoderm deletion (*Hoxa3*$^{fx/-}$;*Foxa2*$^{CreERT2/+}$) embryos (*n*=3) (C,F,G). (F,G) Two different embryos showing the range of *Hoxa3* deletion obtained using *Foxa2*$^{CreERT2}$. Arrows indicate HOXA3-positive cells. Blue staining is DAPI. The third pharyngeal pouch is outlined in all panels. Anterior is towards the top of the image, dorsal is towards the left. Scale bars: 40 µm.

expression of cytokeratin 8 and cytokeratin 5, attracted Ikaros-positive thymocytes (supplementary material Fig. S2C) and showed no increase in CC3-positive apoptotic cells at E12.0 or E13.5 (supplementary material Fig. S2D). Thymus size is thought to be restricted by the initial size of the epithelial progenitor cell pool, and FOXN1 is known to promote TEC proliferation (Su et al., 2003; Bleul et al., 2006; Itoi et al., 2007; Jenkinson et al., 2008; Chen et al., 2009; Griffith et al., 2009; Nowell et al., 2011; Manley et al., 2011). To determine whether delayed *Foxn1* expression or decreased proliferation of *Foxn1*-positive cells was the cause of the thymic hypoplasia, we measured pouch size at E10.5 (before FOXN1 expression) and the proliferation of FOXN1-positive cells at E11.5. Both the size of the third pharyngeal pouch at E10.5 ($P$=0.32633) and the percentage of FOXN1-positive cells that were proliferating at E12.5 (Fig. 6P-R) were similar between the mutant and control thymi. These data are consistent with a model in which the smaller thymus primordium is primarily due to the delay in *Foxn1* expression and the resulting delay in initiation of TEC proliferation, rather than a difference in the number of cells that are initially fated to develop into thymus, an increase in cell death or a decrease in the proliferation of cells that have a thymic fate.

In contrast to the endoderm-specific and null mutant phenotypes, NCC-specific deletion of *Hoxa3* had little effect on the thymus. The timing and pattern of initial *Foxn1* expression was normal (Fig. 6K-N). The newborn mutant thymus was consistently

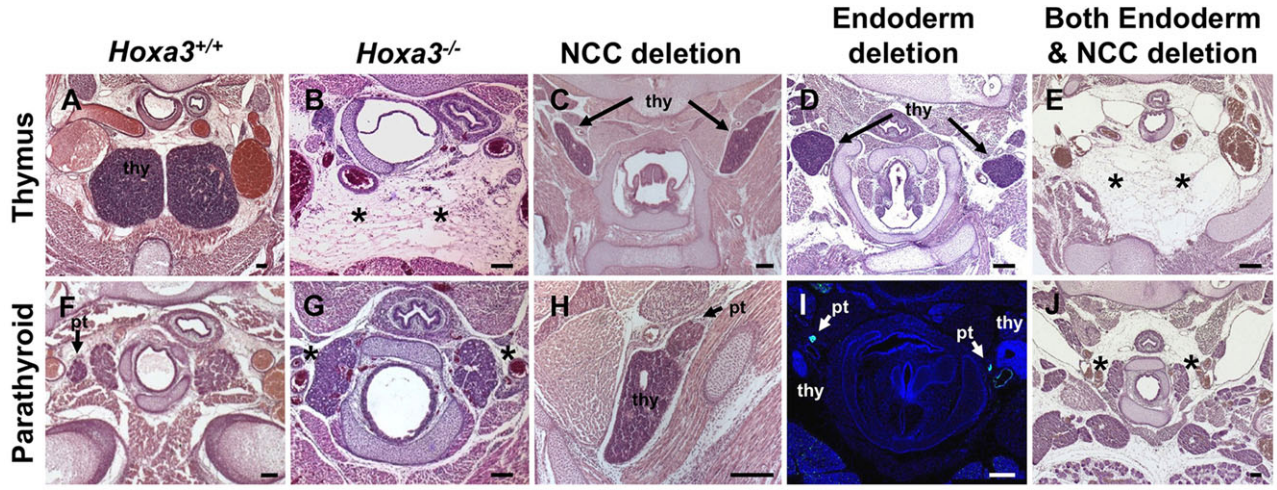


**Fig. 5. The thymus and parathyroids are absent at E17.5 in the *Hoxa3*$^{-/-}$ mutants and after combined tissue-specific deletion, but present after tissue-specific deletion.** H&E staining of transverse sections at E17.5 of *Hoxa3*$^{+/+}$ (A,F), *Hoxa3*$^{-/-}$ (B,G), NCC deletion (*Hoxa3*$^{fx/-}$;*Wnt1Cre*$^{tg/0}$) (*n*=3) (C,H), endoderm deletion (*Hoxa3*$^{fx/-}$;*Foxa2*$^{CreERT2/+}$) (*n*=7) (D), and combined endoderm and NCC deletion (*Hoxa3*$^{fx/-}$;*Foxa2*$^{CreERT2/+}$;*Wnt1Cre*$^{tg/0}$) (*n*=2) (E,J) embryos. (I) An E17.5 transverse section that had been stained with DAPI and imaged for *Gcm2*-EGFP expression (*Hoxa3*$^{fx/-}$;*Foxa2*$^{CreERT2/+}$;*Gcm2-EGFP*) (*n*=2). (J) We were unable to identify parathyroids in the combined deletion mutants. In all sections, dorsal is towards the top of the image. thy, thymus; pt, parathyroid; *, missing organ. Scale bars: 80 µm.

Development (2014) 141, 3697-3708 doi:10.1242/dev.110833

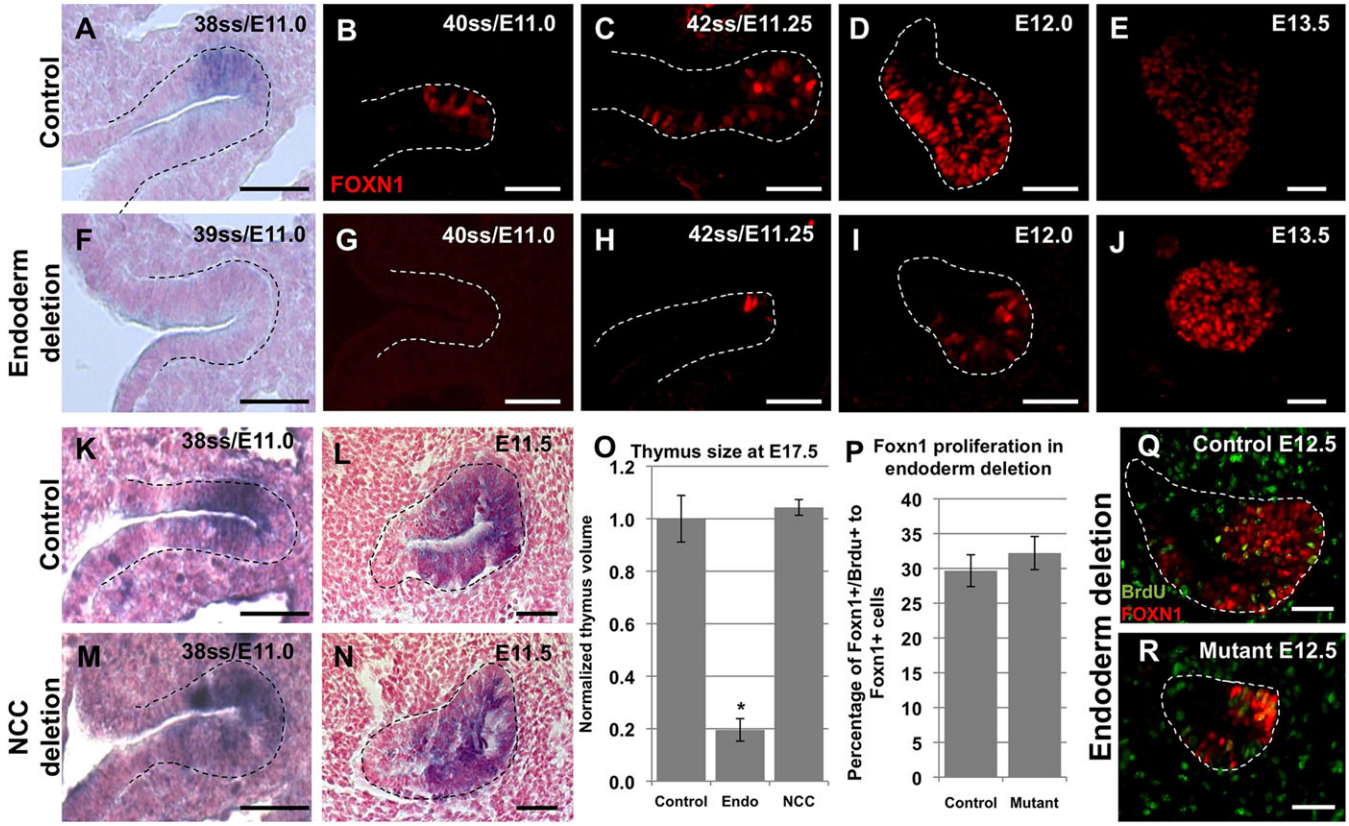


**Fig. 6. Delayed *Foxn1* expression and thymus hypoplasia after endoderm-specific deletion.** Paraffin sections of control (*Hoxa3*$^{+/fx}$;*Foxa2*$^{CreERT2/+}$) and endoderm deletion (*Hoxa3*$^{fx/-}$;*Foxa2*$^{CreERT2/+}$) embryos stained with a *Foxn1* riboprobe using ISH at E11.0 (*n*=2) (A,F) or with an antibody against FOXN1 between E11.0 and E13.5 (*n*=3-5 per stage) (B-E,G-J). (K-N) ISH on paraffin sections from control (*Hoxa3*$^{fx/-}$;*Wnt1Cre*$^{tg/0}$) and NCC deletion (*Hoxa3*$^{fx/-}$;*Wnt1Cre*$^{tg/0}$) embryos for *Foxn1* (*n*=2). (O) Bar chart showing thymus size at E17.5 in the control (*Hoxa3*$^{+/-}$) (*n*=2), and endoderm (Endo) (*Hoxa3*$^{fx/-}$;*Foxa2*$^{CreERT2/+}$) (*n*=3) or NCC deletion mutants (*Hoxa3*$^{fx/-}$;*Wnt1Cre*$^{tg/0}$) (*n*=3). *$P$<0.0001. (P-R) At E12.5, approximately 30% of FOXN1-positive cells were proliferating in both control (*Hoxa3*$^{+/fx}$;*Foxa2*$^{CreERT2/+}$ or *Hoxa3*$^{+/fx}$;*Foxa2*$^{+/+}$) (*n*=3) and endoderm deletion (mutant) (*Hoxa3*$^{fx/-}$; *Foxa2*$^{CreERT2/+}$) (*n*=3) embryos. The third pharyngeal pouch is outlined in all panels. All sections are sagittal and anterior is towards the top of the image. ss, somite stage. Scale bars: 40 µm.

about half the size of littermate controls ($P$=0.033); however, this difference occurred only after E17.5, and we cannot exclude the possibility that the ectopic location restricted its expansion (Fig. 6O; supplementary material Fig. S4A,D). Both thymocyte differentiation (supplementary material Fig. S4B) and TEC marker expression (supplementary material Fig. S4C) appeared to be normal in the newborn mutant thymus. Thus, *Hoxa3* expression in NCCs might be required for postnatal thymus size, but is not required for thymus specification, early organogenesis or TEC differentiation.

### Upregulation of *Gcm2* expression requires endodermal *Hoxa3*

The NCC-specific deletion of *Hoxa3* did not appear to affect *Gcm2* expression at E10.5-E12.5 (Fig. 7I-L; compare I and J,K and L). By contrast, the *Hoxa3* endoderm-specific deletion showed reduced *Gcm2* expression at E10.5 (Fig. 7E,F), similar to that of the *Hoxa3*$^{-/-}$ mutant (Fig. 2M,N; Fig. 7A,B). However, unlike the null mutants, *Gcm2* expression levels increased between E10.5 and E12.0 in the endoderm-specific deletion mutants, such that, by E12.0, *Gcm2* expression was similar to that seen in control embryos at the same stage (Fig. 7C,D,G,H). Closer examination of GCM2 protein levels in the endoderm-specific deletion mutant at E10.5 showed a mosaic pattern reminiscent of the *Foxa2*$^{CreERT2}$ deletion pattern (Fig. 8A,E). These few GCM2-positive cells persisted, forming small clusters of parathyroid cells at E13.5 (Fig. 8D,H) and E17.5 (Fig. 5I). All GCM2-positive cells at E10.5 were also HOXA3-positive, indicating that they probably persist due to the inefficient deletion of *Hoxa3* (Fig. 8A-C,E-G). These results suggest that *Hoxa3* and *Gcm2* are part of a cell-autonomous pathway that promotes parathyroid differentiation. This result is in contrast to the effects of *Hoxa3* deletion on the thymus domain, where cells that never expressed *Hoxa3* were able to express *Foxn1*, albeit with some delay.

### HOXA3 differentially regulates multiple third pharyngeal pouch markers

*Fgf8* and *Bmp4* have regionalized expression patterns in the E10.5 third pharyngeal pouch and are involved in its patterning and differentiation (Gordon and Manley, 2011). *Fgf8* expression overlaps with the presumptive thymus domain at E10.5 in control embryos and in the NCC-specific mutant (Fig. 9A,C; supplementary material Fig. S3C,D). By contrast, *Fgf8* expression expanded into the dorsal pouch in both the *Hoxa3*$^{-/-}$ and *Hoxa3* endoderm-specific deletion embryos (Fig. 9A-D), suggesting that endodermal HOXA3 restricts expression of *Fgf8* to the ventral domain at E10.5. *Bmp4* is usually expressed in both the ventral pouch and the surrounding NCCs at E10.5 and E11.5 (Gordon et al., 2010; see Fig. 9E,G,I,K). Its expression in NCCs was unaffected in the *Hoxa3*$^{-/-}$ mutant or after either endodermal or NCC-specific *Hoxa3* deletion, suggesting that NCC-specific *Bmp4* expression is HOXA3-independent (Fig. 9E-L). *Bmp4* expression in the endoderm was severely reduced in the null compared with the

Development (2014) 141, 3697-3708 doi:10.1242/dev.110833

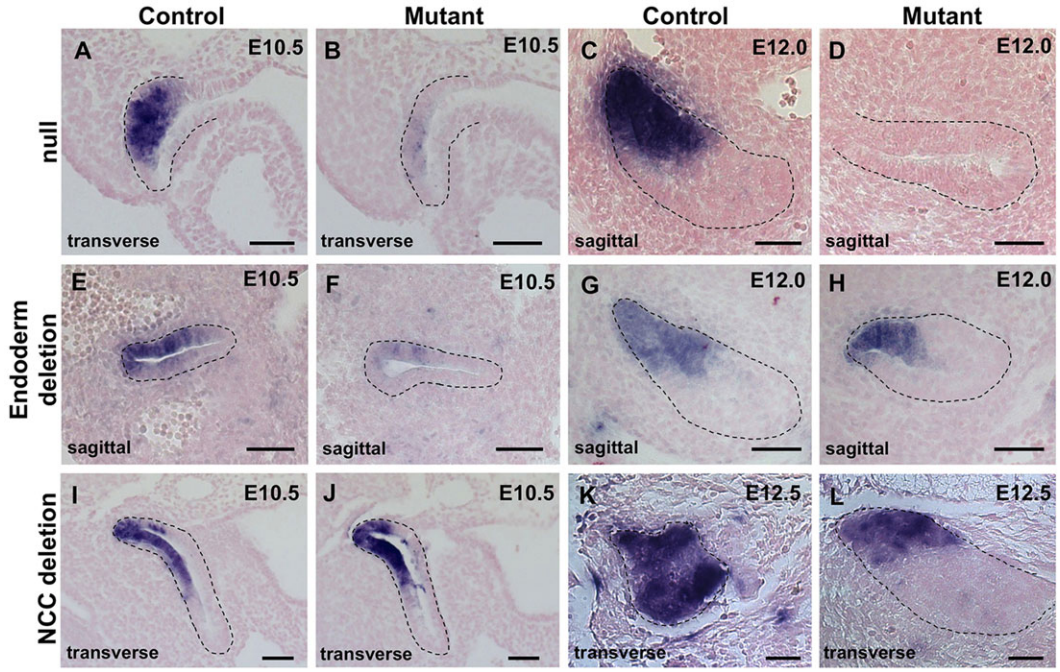


**Fig. 7. *Gcm2* is differentially expressed among the *Hoxa3*$^{-/-}$, NCC deletion and endoderm deletion embryos.** E10.5-E12.5 paraffin sections subjected to ISH with a *Gcm2* riboprobe in different control (*Hoxa3*$^{+/-}$, *Hoxa3*$^{fx/-}$;*Wnt1Cre*$^{0/0}$ or *Hoxa3*$^{fx/+}$;*Foxa2*$^{CreERT2/+}$) embryos, and in null (*Hoxa3*$^{-/-}$), NCC deletion (*Hoxa3*$^{fx/-}$;*Wnt1Cre*$^{tg/0}$) and endoderm deletion (*Hoxa3*$^{fx/-}$;*Foxa2*$^{CreERT2/+}$) embryos (*n*=2-4 per stage, per genotype). The primordium is outlined in all panels. Anterior is towards the top of the image for all sections. Scale bars: 40 µm.

control at E10.5 and was greatly reduced at E11.5. *Bmp4* expression at E10.5 in the endoderm was reduced after endoderm-specific deletion, but normal after NCC deletion of *Hoxa3* (Fig. 9I-L), suggesting that *Hoxa3* expression within the endoderm regulates *Bmp4* expression in the third pharyngeal pouch. The pattern of endodermal *Bmp4* expression in the endoderm-specific deletion mutant could be explained either by delayed expression, similar to that seen for *Foxn1*, or by the *Hoxa3* mosaic deletion that is induced by *Foxa2*$^{CreERT2}$.

## HOXA3 is required in both the endoderm and NCCs for organ separation and migration

Both endoderm and NCCs have been implicated in the detachment of the thymus from the pharynx, the separation of the parathyroid from the thymus and the migration of both organs (Gordon and Manley, 2011). The thymus detaches from the pharynx through coordinated endodermal apoptosis between E11.5 and E12.5. Organ separation and migration occurs between E12.5 and E14.5 and is primarily mediated by NCCs (Gordon et al., 2004; Gordon

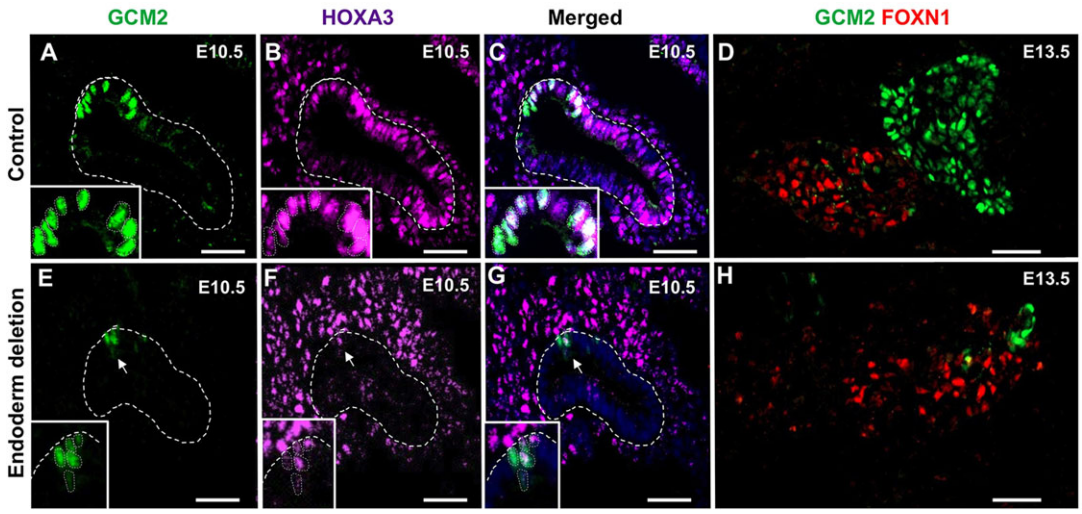


**Fig. 8. GCM2 expression is maintained in cells that fail to delete *Hoxa3* after endoderm-specific deletion.** Sagittal sections of control (*Hoxa3*$^{+/fx}$;*Foxa2*$^{CreERT2/+}$) (A-D) and endoderm deletion (*Hoxa3*$^{fx/-}$;*Foxa2*$^{CreERT2/+}$) (E-H) embryos that had been immunostained with antibodies against GCM2, FOXN1 or HOXA3. The number of GCM2-positive cells was reduced at E10.5 (E, arrows) (*n*=5) and at E13.5 (*n*=2). GCM2 and HOXA3 were co-expressed in E10.5 control and endoderm deletion sections (arrows and insets). For all sections, anterior is towards the top of the image. The third pharyngeal pouch is outlined in all panels. Scale bars: 40 µm.

Development (2014) 141, 3697-3708 doi:10.1242/dev.110833

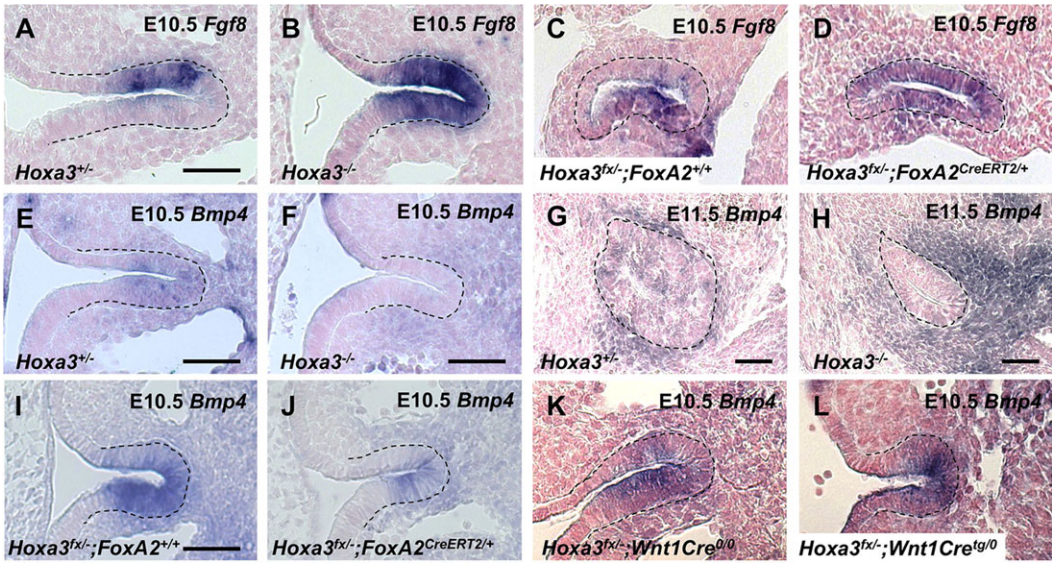


**Fig. 9. Gene expression patterns in the third pharyngeal pouch are affected in the *Hoxa3*$^{-/-}$ mutants and tissue-specific deletions.** E10.5 and E11.5 sagittal paraffin sections from control (*Hoxa3*$^{+/-}$, *Hoxa3*$^{+/fx}$;*Foxa2*$^{+/+}$ and *Hoxa3*$^{fx/-}$;*Wnt1Cre*$^{0/0}$), null (*Hoxa3*$^{-/-}$), NCC deletion (*Hoxa3*$^{fx/-}$;*Wnt1Cre*$^{tg/0}$) and endoderm deletion (*Hoxa3*$^{fx/-}$;*Foxa2*$^{CreERT2/+}$) embryos that had been subjected to ISH with *Fgf8* (A-D) and *Bmp4* (E-L) riboprobes (*n*=2-3 per stage, per genotype). In all sections, anterior is towards the top of the image. Scale bars: 40 µm. The scale bar in A is representative for B-D and that in I is representative for J-L.

and Manley, 2011; Gardiner et al., 2012). None of these events occurred in the *Hoxa3*$^{-/-}$ mutant, as the entire primordium was undergoing apoptosis before and during the stages at which these events normally occur (Fig. 3E,F). After endoderm-specific deletion of *Hoxa3*, separation of the thymus from the parathyroids appeared to occur normally (Fig. 5I), but detachment from the pharynx was delayed until E14.5 (supplementary material Fig. S5A,B,D,E). This delay resulted in delayed migration, making the final location of the mutant thymi variable among mutant embryos and between the two sides of the same embryo. By contrast, the NCC-specific deletion mutant thymus never detached from the pharynx, and the mutant embryos had fewer TUNEL-positive cells within the endoderm compared with control embryos (supplementary material Fig. S5C,F). The thymus and parathyroids also remained connected to each other at least until the newborn stage (supplementary material Fig. S5G,H).

### HOXA3 is not required for later maintenance of thymic epithelial cells or parathyroids

To test whether HOXA3 is required at later stages in the development of the thymus and parathyroids, we generated conditional mutants using *Foxn1*$^{Cre}$ to drive deletion in embryonic TECs (Gordon et al., 2007) or a *PthCre* transgene to drive deletion in the embryonic parathyroid (Libutti et al., 2003). Both Cre lines efficiently drive deletion beginning around E11.5, after organ fate has been established and differentiation has initiated. Each deletion had little or no effect on later organ phenotypes. Deletion of *Hoxa3* using *PthCre* showed no change in parathyroid size relative to controls (1:1 volume ratio at E15.5, E16.5 and E18.5, *n*=2 for each stage), and *Pth* and *Gcm2* exhibited normal expression patterns at E13.5 (supplementary material Fig. S6). No significant changes were seen in the postnatal thymus after *Hoxa3* deletion using *Foxn1*$^{Cre}$ (supplementary material Fig. S7). Cortical and medullary differentiation and organization were similar to those in controls at the newborn stage (supplementary material Fig. S7B), and T-cell development was unaffected (supplementary material Fig. S7C). Because the paralogous gene *Hoxd3* is also expressed in cortical TECs (supplementary material Fig. S7D) and *Hoxd3* has multiple redundant functions with *Hoxa3* (Condie and Capecchi, 1994; Manley and Capecchi, 1997, 1998), we removed one copy of the *Hoxd3* allele in the homozygous *Hoxa3* TEC-specific conditional mutants (*Hoxd3*$^{+/-}$;*Hoxa3*$^{fx/-}$;*Foxn1*$^{Cre/+}$). Results were similar to the *Hoxa3* conditional mutant (supplementary material Fig. S7B). Therefore, *Hoxa3* expression is not necessary for the normal development or function of TECs or parathyroids after E11.5.

## DISCUSSION

Our current data show that HOXA3 does not establish third pharyngeal regional identity, but is instead required in both pharyngeal endoderm and NCCs for patterning and early organogenesis of the thymus and parathyroids. Using tissue-specific *Hoxa3* deletions, we establish that *Hoxa3* expression in the endoderm has independent roles in early third pharyngeal pouch patterning, parathyroid differentiation and the temporal regulation of thymus-specific markers. Deletion of *Hoxa3* in one or all tissues results in changes to apoptosis, with HOXA3 either promoting or blocking cell death in different aspects of organogenesis. The role of HOXA3 in TEC survival is redundant between the endoderm and NCCs as *Hoxa3* must be deleted from both cell types simultaneously for the thymus to undergo apoptosis. By contrast, *Hoxa3* deletion in either cell type causes defects in the morphogenesis of the third pharyngeal pouch-derived organs. HOXA3 function is primarily restricted to early organogenesis because the loss of *Hoxa3* after organ fate was established had very little effect on thymus or parathyroid development.

### *Hoxa3* regulates parathyroid differentiation and survival in a cell-autonomous manner

*Hoxa3* deletion resulted in several gene expression changes within the parathyroid domain. The key change is the failure to upregulate *Gcm2*. *Gcm2* regulates parathyroid differentiation and survival; in the *Gcm2*$^{-/-}$ mutant, the parathyroid domain is specified, but fails

Development (2014) 141, 3697-3708 doi:10.1242/dev.110833

to turn on *Pth*, and undergoes coordinated apoptosis at E12-12.5 (Liu et al., 2007). This phenotype is similar to the null mutant and *Hoxa3* endoderm-specific deletion phenotypes; thus, the simplest interpretation is that the differentiation failure and ultimate parathyroid loss are caused by loss of *Gcm2*. Our data also suggest that *Gcm2* is upregulated in a HOXA3-directed cell-autonomous manner (evidenced by the few *Hoxa3 Gcm2* double-positive cells after endoderm-specific deletion), but once *Gcm2* is upregulated, HOXA3 is not required for its expression or for parathyroid differentiation or maintenance.

HOXA3 appears to repress *Fgf8*, *p63* and *Foxg1* in the parathyroid domain, as all three are ectopically expressed following *Hoxa3* deletion; however, *Bmp4* and *Foxn1* were not expressed in this domain at any time. These genes have all been implicated in thymus fate determination (Manley et al., 2011). *Gcm2* and *Tbx1* expression, normally restricted to the parathyroid domain, was reduced, but still initiated in this domain. Thus, in the absence of HOXA3, the dorsal-anterior domain cells express a subset of markers that are characteristic of both fates and fail to establish either the parathyroid or the thymus fate.

### *Hoxa3* is not the initiator of the thymus program

In the thymus domain, HOXA3 appears to regulate the timing of the thymus-specific program, but is not required for its execution. *Fgf8* and *p63* expression are not affected in the thymus domain by loss of *Hoxa3* (although they expand dorsally, it is unclear at this point how HOXA3 differentially affects the expression of a single gene in the dorsal versus ventral pouch). Expression of the thymus markers *Bmp4*, *Foxg1* and *Foxn1* is delayed by at least a day. The loss of *Bmp4* in the endoderm in the null mutant could be especially significant; studies in the chick system have shown that *Bmp4* expression from the mesenchyme is required for *Foxn1* expression (Neves et al., 2012). The persistence of *Bmp4* in the mesenchyme could be the signal that allows *Foxn1* expression, albeit delayed, in the *Hoxa3* null and endoderm-deletion mutants. In chick, this role for *Bmp4* is mediated in part through induction of *Fgf10* expression, but as *Fgf10* is not expressed in the mesenchyme at these stages in mice, this pathway appears to be operating differently. Furthermore, as *Fgf8* expansion does not induce ectopic *Bmp4* expression in the dorsal domain, and is usually expressed in the ventral domain where *Bmp4* is delayed, *Fgf8* and *Bmp4* appear to be independently regulated.

The delayed thymus program appears to be a *Hoxa3* endoderm-specific function because the delay occurs in a manner similar to that in the endoderm-specific deletion mutant, with the apparent exception of the few HOXA3-positive 'escapers' that might become FOXN1-positive first (supplementary material Fig. S2B). Because there are also HOXA3-positive FOXN1-negative cells in the same mutant (supplementary material Fig. S2B), HOXA3 is not sufficient to induce *Foxn1* expression, unlike expression of *Gcm2*. It is possible that the local concentration of BMP4 (from both reduced expression in the endoderm and the surrounding NCCs) must be sufficiently high to activate a 'community' effect. However, all cells eventually turn on *Foxn1*, even in the null mutants that never express *Hoxa3*. Thus, the overall effect of *Hoxa3* loss is to slow the progression of this 'thymus program', suggesting that HOXA3 potentiates, but is not required for, its execution. Thus, the transcriptional initiator of the thymus program remains unknown.

### *Hoxa3* regulates thymus and parathyroid survival in different ways

HOXA3 uses two independent mechanisms to protect the parathyroid and thymus cells from cell death. The most straightforward case is in the parathyroid, where HOXA3 upregulates *Gcm2*, which in turn protects those cells from cell death. In this model, the role of *Hoxa3* in parathyroid survival is a consequence of its role in regulating the differentiation program.

The loss of the thymus due to cell death in the *Hoxa3*$^{-/-}$ mutants presents a more complex role for HOXA3 in cell survival. Thymus survival is controlled by HOXA3 acting in both NCCs and endoderm, where expression in either cell type is sufficient to promote organ survival. This requirement for HOXA3 appears to be restricted to before E11.5-E12, as *Hoxa3* expression in wild-type embryos declines throughout the time of cell death in the null (E11.5-E13.5) and all tissue-specific and organ-specific deletions form a functioning thymus. Unlike in parathyroids, this survival program is an independent HOXA3 function that acts in parallel to its role in TEC differentiation. TEC death initiates at E11.5 before the delayed *Foxn1* expression in the mutants and continues through E13, during which TECs continue to acquire expression of *Foxn1* and other TEC markers. The simplest model is that HOXA3 promotes the expression of survival signals in both the endoderm and NCCs, with either source being sufficient for survival; the receptor for the survival signal could be HOXA3-independent (Fig. 10). In the simplest case, the survival signal is the same in both cell types; however, this is not required. This thymus-specific survival signal must act through a threshold effect because the *Hoxa3*-expressing 'escaper' cells after *Hoxa3* deletion from both the NCCs and the endoderm do not survive.

### Separation and migration of the thymus and parathyroid

Between E12 and E14, the thymus and parathyroids detach from the pharyngeal endoderm, separate from each other and migrate to their final position in the adult animal. All three events are mechanistically different; however, organ separation and migration both depend on proper detachment, which occurs through coordinated apoptosis of the endoderm at about E12 (Gordon and Manley, 2011). This regional apoptosis is absent in the null mutant, suggesting that the role of HOXA3 in this process is to promote apoptosis, in contrast to its role in promoting cell survival in TECs. As both endoderm- and NCC-specific deletions of *Hoxa3* have defective detachment from the pharynx, HOXA3 is independently required in both tissues for this

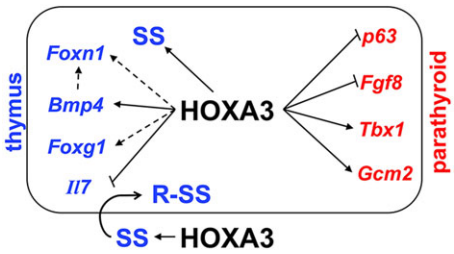


**Fig. 10. Model and summary of HOXA3 function in the third pharyngeal pouch at E10.5-E11.5.** The box represents the endodermal primordium, with the ventral thymus and dorsal parathyroid domains indicated. In the parathyroid domain (red), HOXA3 represses *Fgf8* and *p63* expression, and upregulates *Tbx1* and *Gcm2*. Once upregulated, *Gcm2* is sufficient to promote parathyroid differentiation and survival independent of HOXA3. In the thymus domain (blue), HOXA3 is required for *Bmp4* expression, and potentiates *Foxg1* and *Foxn1* expression (dashed lines), both of which are delayed in the absence of *Hoxa3*. *Il7* expression is upregulated in *Hoxa3*$^{-/-}$ mice. BMP4 has also been implicated in regulating *Foxn1* in other studies, although it is not required. We propose that HOXA3 upregulates a thymus-specific survival signal (SS) in both the endoderm and NCC (outside of the box); the receptor for this signal (R-SS) in the endoderm is HOXA3-independent.

Development (2014) 141, 3697-3708 doi:10.1242/dev.110833

process. The role in NCCs appears paramount, as detachment fails completely after NCC-specific deletion, whereas it is only delayed after endoderm-specific deletion. Because apoptosis is only reduced, but not absent, after NCC-specific deletion, we propose that HOXA3 controls a pro-apoptotic signal in both NCCs and endoderm that acts on the endoderm in an additive or combinatorial fashion to promote a sufficient amount of cell death to result in detachment. In the absence of either source of this signal, cell death is reduced below the threshold needed for correct detachment, with the NCC-specific source being most important.

The identity of this pro-apoptotic signal is unclear – both SHH and inhibition of FGF signaling have been implicated in promoting this cell death; it is also unclear how these signaling pathways interact in this process (Moore-Scott and Manley, 2005; Basson et al., 2008). Increased FGF signaling through loss of SPRY inhibitors results in a failure of detachment that looks remarkably similar to the *Hoxa3* NCC-specific deletion (Basson et al., 2008). Although the *Hoxa3*$^{-/-}$ and endoderm-specific deletion mutants both have ectopic *Fgf8* expression in the dorsal pouch, this ectopic expression is limited to E10.5; before this, apoptosis and SHH signaling are unaffected by loss of *Hoxa3*. Thus, although these signaling pathways might be involved in this aspect of the *Hoxa3* mutant phenotype, the structure of the network that mediates this function has yet to be definitively identified.

## MATERIALS AND METHODS

### Generation of mice and genotype analysis

*Foxa2*$^{CreERT2}$ (Park et al., 2008), *Wnt1Cre* (Danielian et al., 1998), *PthCre* (Libutti et al., 2003), *Foxn1Cre* (Gordon et al., 2007), *Ptch1*$^{LacZ}$ (Goodrich et al., 1997), *Gcm2*-EGFP (Gong et al., 2003), *Hoxd3*$^{null}$ (Condie and Capecchi, 1993) and *Hoxa3*$^{null}$ (Chisaka and Capecchi, 1991; and described below) mouse strains were maintained and genotyped as described previously. The *Hoxa3*$^{fx}$ conditional allele (supplementary material Fig. S1) was maintained as a homozygous colony. *Gcm2*-EGFP transgenic mice were obtained from the Mutant Mouse Regional Research Center (MMRRC) [STOCK Tg(Gcm2-EGFP)FG26Gsat/Mmucd; Stock no. 011818-UCD). All colonies were maintained on a majority C57BL6/J genetic background.

The original *Hoxa3*$^{null}$ carries a neomycin resistance (neo$^{r}$) gene cassette that has been inserted within the homeodomain in exon 2 (Chisaka and Capecchi, 1991). As some cassette-containing alleles influence neighboring gene expression, we generated a new null allele, deleting the second coding exon in the germ line using a *Hoxa3*$^{fx}$ conditional allele and B6Cg-Tg(TeK-Cre)12Flv/J (Stock no. 004128) (Koni et al., 2001). This new null allele had neither detectable *Hoxa3* mRNA nor protein (Fig. 2; supplementary material Fig. S1D) and was phenotypically comparable to the original allele. Both alleles were used throughout this paper; for simplicity we refer to both as *Hoxa3*$^{-/-}$. The following primers were used to PCR genotype this allele: forward, 5′-TCTGTCTCTCCCCCTCAAAGTGCCAACAGCAACCC-3′; forward, 5′-AGTAACCAAAGAAGGTCGGGTGGGCAACTCTCCTG-3′; reverse, 5′-ACTCTTTGGCCTAACTCACCTC-3′.

Conditional mutants were generated by crossing *Hoxa3*$^{fx/fx}$ females with *Hoxa3*$^{+/-}$*;Cre/+* males, generating heterozygous embryos that were homozygous null only in the target tissues. Embryonic age was estimated as noon of the day of a vaginal plug as E0.5; stages were confirmed by somite number and morphology. The *Foxa2*$^{CreERT2}$ allele was activated by single intraperitoneal injections of 3 mg tamoxifen (Sigma-Aldrich) in sterile corn oil (Sigma-Aldrich) per 40 g of mouse weight into gravid females at E6.5 (Hayashi et al., 2002), or serial injections at E5.5 and E6.5 (supplementary material Fig. S2A). Yolk sac or tail DNA was genotyped by PCR. Embryos or newborns carrying tissue-specific deletions (*fx/−;Cre/+*) were termed 'mutant'. Both *+/fx;Cre/+* and *+/fx;+/+* embryos were used as controls and were indistinguishable in all assays. All experiments involving animals were performed with approval of the University of Georgia, Athens, Institutional Animal Care and Use Committee.

### mRNA quantification

Total mRNA was isolated from embryos at E10.5, followed by reverse transcription using Superscript II (Invitrogen). cDNA was used as a template for relative quantification of *Hoxa3* (Mm01326402_m1), *Hprt* (Mm01545399_m1) and *Tbp* (Mm01277042_m1) (Applied Biosystems) using commercially available reagents (Invitrogen) on an Applied Biosystems 7500 Real Time PCR System. Three mutant and control embryos were run individually in duplicate; a control reaction lacking reverse transcriptase was also performed. Analysis was performed by relative quantification using the comparative $C_t$ method. Both reference genes gave similar results; *Tbp* results are shown.

### Histology and three-dimensional reconstructions

Standard hematoxylin and eosin (H&E) histological staining was performed on transverse paraffin sections of embryos and newborns. Between two and five embryos (e.g. 4-10 primordia) were analyzed for each stage and genotype; representative images are shown. *n*-values are in the text and figure legends. Three-dimensional reconstructions were generated from images of serial H&E-stained sections from three E17.5 embryos per genotype using Surf Driver 3.5.3. Thymus size was calculated as the volume of each reconstruction using the Volumetrics function.

### X-gal staining and *in situ* hybridization

X-gal staining was performed on E10.5 *Ptch1LacZ* embryos as described (DasGupta and Fuchs, 1999). Section *in situ* hybridization (ISH) was performed as described previously (Carpenter et al., 1993; Manley and Capecchi, 1995). Two to three embryos were used for each genotype and probe. Probes for *Bmp4* (Jones et al., 1991), *Fgf8* (Crossley and Martin, 1995), *Foxg1* (Wei and Condie, 2011), *Foxn1* (Gordon et al., 2001), *Gcm2* (Gordon et al., 2001), *Hoxa3* (Manley and Capecchi, 1995), *Il7* (Zamisch et al., 2005), *Pth* (Liu et al., 2007) and *Tbx1* (Chapman et al., 1996) have been previously described.

### Immunohistochemistry

IHC was performed on sectioned (7 µm) paraffin-embedded or frozen embryos fixed in 4% paraformaldehyde (PFA). Paraffin-embedded tissue was de-waxed in xylene and rehydrated through an ethanol gradient to $dH_2O$ and then boiled in antigen-retrieval buffer (10 mM $Na_3$Citrate pH 6, 0.05% Tween20) for 30 min. Slides were incubated overnight in primary antibody, 10% donkey serum and PBS at 4°C, washed in PBS and then incubated with secondary antibody in PBS for 30 min at room temperature in the dark. Slides were washed in PBS containing DAPI at 1:10,000, and mounted with EMS-Fluorogel. Antibodies recognized FOXN1 (Santa Cruz G-20), GCM2 (Abcam), cleaved caspase-3 (CC3; Cell Signaling), BrdU (Serotec), Ikaros (Santa Cruz, M-20), pan-cytokeratin (Sigma-Aldrich), keratin 5 (Covance), keratin 14 (Covance), PDGFRβ (BD Biosciences), keratin 8 (ProGene), HOXA3 (Santa Cruz, F-7) or ΔNP63 (Abcam). Secondary antibodies were DyLight-conjugated (Jackson Immunoresearch). Biotinylated UEA-1 lectin was detected with streptavidin (Vector Labs). Images were acquired using a Zeiss LSM510 confocal microscope and image acquisition software.

### Apoptosis, proliferation and primordium size

The terminal deoxynucleotidyl transferase dUTP nick end labeling (TUNEL) assay was performed following the manufacturer's guidelines (Roche Diagnostics). E11.5 embryos were fixed in 4% PFA for 1 h, embedded in paraffin and sectioned (7 µm).

For proliferation analysis, gravid females were injected with 50 mg BrdU per kg body weight. E12.5 embryos were collected 75 min later and processed for BrdU and FOXN1 IHC. FOXN1-positive cells and FOXN1 BrdU double-positive cells were counted manually and the percentage of double-positive cells was calculated per lobe. Values were averaged for both lobes per embryo, and those values were averaged for three embryos per genotype.

To calculate primordium size, three E10.5 embryos each for the endoderm deletion mutant and control were serially sectioned in the sagittal plane and stained with DAPI. Primordium area was measured using the trace tool in AxioVision 4.8.2 (Zeiss). Volumes were calculated per thymus.

Development (2014) 141, 3697-3708 doi:10.1242/dev.110833

### Thymocyte analysis

Thymocytes were harvested from minced newborn thymi and the total cell number calculated per embryo (two lobes each). Cells were suspended in 1× FACS buffer (1× PBS with 2% BSA and 0.1% $NaN_3$) and incubated with the following conjugated monoclonal antibodies: anti-CD4 APC (GK1.5), anti-CD8 FITC (53-6.7), anti-ckit-PE (2B8) and anti-CD25 biotin (3C7), followed by streptavidin-PerCP. Cells were incubated at 4°C for 30 min, washed and fixed with 1% PFA before flow cytometric analysis using a FACS Caliber instrument (Becton Dickinson). Data were analyzed with CellQuest software.

### Statistics

Data are presented as the mean±s.d. Comparisons were analyzed using Student's *t*-test or the Wilcoxon rank-sum test where appropriate; $P<0.05$ was considered significant.

#### Acknowledgements

We thank Paola LaSanta-Ortiz for technical assistance and Julie Gordon and Brian Condie for project advice. We thank Julie Nelson in the University of Georgia Center for Tropical and Emerging Global Diseases Flow Cytometry Facility. We thank Ellen Richie, Jonathan Eggenschwiler, Scott Dougan and Jim Lauderdale for reading the manuscript before submission.

#### Competing interests

The authors declare no competing financial interests.

#### Author contributions

N.R.M. and J.L.C. designed the study; J.L.C., K.M. and H.A.T. performed experiments; N.R.M., J.L.C., K.M. and H.A.T. performed data analysis; K.T. and M.C. generated the conditional *Hoxa3* strain; N.R.M. and J.L.C. prepared the manuscript; and all authors contributed to editing the manuscript prior to submission.

#### Funding

This work was supported by internal funding from the University of Georgia Office of the Vice President for Research (OVPR). The conditional strain was developed in the Capecchi lab funded by the Howard Hughes Medical Institute (HHMI). Deposited in PMC for release after 6 months.

#### Supplementary material

Supplementary material available online at http://dev.biologists.org/lookup/suppl/doi:10.1242/dev.110833/-/DC1

#### References

**Basson, M. A., Echevarria, D., Petersen Ahn, C., Sudarov, A., Joyner, A. L., Mason, I. J., Martinez, S. and Martin, G. R.** (2008). Specific regions within the embryonic midbrain and cerebellum require different levels of FGF signaling during development. *Development* **135**, 889-898.

**Bleul, C. C. and Boehm, T.** (2005). BMP signaling is required for normal thymus development. *J. Immunol.* **175**, 5213-5221.

**Bleul, C. C., Corbeaux, T., Reuter, A., Fisch, P., Mönting, J. S. and Boehm, T.** (2006). Formation of a functional thymus initiated by a postnatal epithelial progenitor cell. *Nature* **441**, 992-996.

**Carpenter, E. M., Goddard, J. M., Chisaka, O., Manley, N. R. and Capecchi, M. R.** (1993). Loss of Hox-A1 (Hox-1.6) function results in the reorganization of the murine hindbrain. *Development* **118**, 1063-1075.

**Chapman, D. L., Garvey, N., Hancock, S., Alexiou, M., Agulnik, S. I., Gibson-Brown, J. J., Cebra-Thomas, J., Bollag, R. J., Silver, L. M. and Papaioannou, V. E.** (1996). Expression of the T-box family genes, Tbx1-Tbx5, during early mouse development. *Dev. Dyn.* **206**, 379-390.

**Chen, L., Xiao, S. and Manley, N. R.** (2009). Foxn1 is required to maintain the postnatal thymic microenvironment in a dosage-sensitive manner. *Blood* **113**, 567-574.

**Chen, L., Zhao, P., Wells, L., Amemiya, C. T., Condie, B. G. and Manley, N. R.** (2010). Mouse and zebrafish Hoxa3 orthologues have nonequivalent in vivo protein function. *Proc. Natl. Acad. Sci. USA* **107**, 10555-10560.

**Chisaka, O. and Capecchi, M. R.** (1991). Regionally restricted developmental defects resulting from targeted disruption of the mouse homeobox gene *hox-1.5*. *Nature* **350**, 473-479.

**Condie, B. G. and Capecchi, M. R.** (1993). Mice homozygous for a targeted disruption of Hoxd-3 (Hox-4.1) exhibit anterior transformations of the first and second cervical vertebrae, the atlas and the axis. *Development* **119**, 579-595.

**Condie, B. G. and Capecchi, M. R.** (1994). Mice with targeted disruptions in the paralogous genes hoxa-3 and hoxd-3 reveal synergistic interactions. *Nature* **370**, 304-307.

**Crossley, P. H. and Martin, G. R.** (1995). The mouse Fgf8 gene encodes a family of polypeptides and is expressed in regions that direct outgrowth and patterning in the developing embryo. *Development* **121**, 439-451.

**Danielian, P. S., Muccino, D., Rowitch, D. H., Michael, S. K. and McMahon, A. P.** (1998). Modification of gene activity in mouse embryos in utero by a tamoxifen-inducible form of Cre recombinase. *Curr. Biol.* **8**, 1323-1326.

**DasGupta, R. and Fuchs, E.** (1999). Multiple roles for activated LEF/TCF transcription complexes during hair follicle development and differentiation. *Development* **126**, 4557-4568.

**Frank, D. U., Fotheringham, L. K., Brewer, J. A., Muglia, L. J., Tristani-Firouzi, M., Capecchi, M. R. and Moon, A. M.** (2002). An Fgf8 mouse mutant phenocopies human 22q11 deletion syndrome. *Development* **129**, 4591-4603.

**Gardiner, J. R., Jackson, A. L., Gordon, J., Lickert, H., Manley, N. R. and Basson, M. A.** (2012). Localised inhibition of FGF signalling in the third pharyngeal pouch is required for normal thymus and parathyroid organogenesis. *Development* **139**, 3456-3466.

**Garg, V., Yamagishi, C., Hu, T., Kathiriya, I. S., Yamagishi, H. and Srivastava, D.** (2001). Tbx1, a DiGeorge syndrome candidate gene, is regulated by sonic hedgehog during pharyngeal arch development. *Dev. Biol.* **235**, 62-73.

**Gaufo, G. O., Thomas, K. R. and Capecchi, M. R.** (2003). Hox3 genes coordinate mechanisms of genetic suppression and activation in the generation of branchial and somatic motoneurons. *Development* **130**, 5191-5201.

**Gaunt, S. J.** (1987). Homeobox gene *Hox1.5* expression in mouse embryos: earliest detection by in situ hybridization is during gastrulation. *Development* **101**, 51-60.

**Gaunt, S. J.** (1988). Mouse homeobox gene transcripts occupy different but overlapping domains in embryonic germ layers and organs: a comparison of Hox-3.1 and Hox-1.5. *Development* **103**, 135-144.

**Gong, S., Zheng, C., Doughty, M. L., Losos, K., Didkovsky, N., Schambra, U. B., Nowak, N. J., Joyner, A., Leblanc, G., Hatten, M. E. et al.** (2003). A gene expression atlas of the central nervous system based on bacterial artificial chromosomes. *Nature* **425**, 917-925.

**Goodrich, L. V., Milenković, L., Higgins, K. M. and Scott, M. P.** (1997). Altered neural cell fates and medulloblastoma in mouse patched mutants. *Science* **277**, 1109-1113.

**Gordon, J. and Manley, N. R.** (2011). Mechanisms of thymus organogenesis and morphogenesis. *Development* **138**, 3865-3878.

**Gordon, J., Bennett, A. R., Blackburn, C. C. and Manley, N. R.** (2001). Gcm2 and Foxn1 mark early parathyroid- and thymus-specific domains in the developing third pharyngeal pouch. *Mech. Dev.* **103**, 141-143.

**Gordon, J., Wilson, V. A., Blair, N. F., Sheridan, J., Farley, A., Wilson, L., Manley, N. R. and Blackburn, C. C.** (2004). Functional evidence for a single endodermal origin for the thymic epithelium. *Nat. Immunol.* **5**, 546-553.

**Gordon, J., Xiao, S., Hughes, B., Su, D.-M., Navarre, S. P., Condie, B. G. and Manley, N. R.** (2007). Specific expression of lacZ and cre recombinase in fetal thymic epithelial cells by multiplex gene targeting at the Foxn1 locus. *BMC Dev. Biol.* **7**, 69.

**Gordon, J., Patel, S. R., Mishina, Y. and Manley, N. R.** (2010). Evidence for an early role for BMP4 signaling in thymus and parathyroid morphogenesis. *Dev. Biol.* **339**, 141-154.

**Grevellec, A., Graham, A. and Tucker, A. S.** (2011). Shh signalling restricts the expression of Gcm2 and controls the position of the developing parathyroids. *Dev. Biol.* **353**, 194-205.

**Griffith, A. V., Cardenas, K., Carter, C., Gordon, J., Iberg, A., Engleka, K., Epstein, J. A., Manley, N. R. and Richie, E. R.** (2009). Increased thymus- and decreased parathyroid-fated organ domains in Splotch mutant embryos. *Dev. Biol.* **327**, 216-227.

**Günther, T., Chen, Z.-F., Kim, J., Priemel, M., Rueger, J. M., Amling, M., Moseley, J. M., Martin, T. J., Anderson, D. J. and Karsenty, G.** (2000). Genetic ablation of parathyroid glands reveals another source of parathyroid hormone. *Nature* **406**, 199-203.

**Hayashi, S., Lewis, P., Pevny, L. and McMahon, A. P.** (2002). Efficient gene modulation in mouse epiblast using a Sox2Cre transgenic mouse strain. *Gene Expr. Patterns* **2**, 93-97.

**Itoi, M., Tsukamoto, N. and Amagai, T.** (2007). Expression of Dll4 and CCL25 in Foxn1-negative epithelial cells in the post-natal thymus. *Int. Immunol.* **19**, 127-132.

**Jenkinson, W. E., Bacon, A., White, A. J., Anderson, G. and Jenkinson, E. J.** (2008). An epithelial progenitor pool regulates thymus growth. *J. Immunol.* **181**, 6101-6108.

**Jones, C. M., Lyons, K. M. and Hogan, B. L.** (1991). Involvement of Bone Morphogenetic Protein-4 (BMP-4) and Vgr-1 in morphogenesis and neurogenesis in the mouse. *Development* **111**, 531-542.

**Kameda, Y., Nishimaki, T., Takeichi, M. and Chisaka, O.** (2002). Homeobox gene hoxa3 is essential for the formation of the carotid body in the mouse embryos. *Dev. Biol.* **247**, 197-209.

**Kameda, Y., Watari-Goshima, N., Nishimaki, T. and Chisaka, O.** (2003). Disruption of the Hoxa3 homeobox gene results in anomalies of the carotid artery system and the arterial baroreceptors. *Cell Tissue Res.* **311**, 343-352.

Development (2014) 141, 3697-3708 doi:10.1242/dev.110833

**Kameda, Y., Arai, Y., Nishimaki, T. and Chisaka, O.** (2004). The role of Hoxa3 gene in parathyroid gland organogenesis of the mouse. *J. Histochem. Cytochem.* **52**, 641-651.

**Koni, P. A., Joshi, S. K., Temann, U.-A., Olson, D., Burkly, L. and Flavell, R. A.** (2001). Conditional vascular cell adhesion molecule 1 deletion in mice: impaired lymphocyte migration to bone marrow. *J. Exp. Med.* **193**, 741-754.

**Libutti, S. K., Crabtree, J. S., Lorang, D., Burns, A. L., Mazzanti, C., Hewitt, S. M., O'Connor, S., Ward, J. M., Emmert-Buck, M. R., Remaley, A. et al.** (2003). Parathyroid gland-specific deletion of the mouse Men1 gene results in parathyroid neoplasia and hypercalcemic hyperparathyroidism. *Cancer Res.* **63**, 8022-8028.

**Liu, Z., Yu, S. and Manley, N. R.** (2007). Gcm2 is required for the differentiation and survival of parathyroid precursor cells in the parathyroid/thymus primordia. *Dev. Biol.* **305**, 333-346.

**Mallo, M., Wellik, D. M. and Deschamps, J.** (2010). Hox genes and regional patterning of the vertebrate body plan. *Dev. Biol.* **344**, 7-15.

**Manley, N. R. and Capecchi, M. R.** (1995). The role of Hoxa-3 in mouse thymus and thyroid development. *Development* **121**, 1989-2003.

**Manley, N. R. and Capecchi, M. R.** (1997). Hox group 3 paralogous genes act synergistically in the formation of somitic and neural crest-derived structures. *Dev. Biol.* **192**, 274-288.

**Manley, N. R. and Capecchi, M. R.** (1998). Hox group 3 paralogs regulate the development and migration of the thymus, thyroid, and parathyroid glands. *Dev. Biol.* **195**, 1-15.

**Manley, N. R. and Condie, B. G.** (2010). Transcriptional regulation of thymus organogenesis and thymic epithelial cell differentiation. *Prog. Mol. Biol. Transl. Sci.* **92**, 103-120.

**Manley, N. R., Richie, E. R., Blackburn, C. C., Condie, B. G. and Sage, J.** (2011). Structure and function of the thymic microenvironment. *Front. Biosci.* **17**, 2461-2477.

**Moore-Scott, B. A. and Manley, N. R.** (2005). Differential expression of Sonic hedgehog along the anterior-posterior axis regulates patterning of pharyngeal pouch endoderm and pharyngeal endoderm-derived organs. *Dev. Biol.* **278**, 323-335.

**Nehls, M., Pfeifer, D., Schorpp, M., Hedrich, H. and Boehm, T.** (1994). New member of the winged-helix protein family disrupted in mouse and rat nude mutations. *Nature* **372**, 103-107.

**Nehls, M., Kyewski, B., Messerle, M., Waldschütz, R., Schüddekopf, K., Smith, A. J. H. and Boehm, T.** (1996). Two genetically separable steps in the differentiation of thymic epithelium. *Science* **272**, 886-889.

**Neves, H., Dupin, E., Parreira, L. and Le Douarin, N. M.** (2012). Modulation of Bmp4 signalling in the epithelial-mesenchymal interactions that take place in early thymus and parathyroid development in avian embryos. *Dev. Biol.* **361**, 208-219.

**Nowell, C. S., Bredenkamp, N., Tetélin, S., Jin, X., Tischner, C., Vaidya, H., Sheridan, J. M., Stenhouse, F. H., Heussen, R., Smith, A. J. H. et al.** (2011). Foxn1 regulates lineage progression in cortical and medullary thymic epithelial cells but is dispensable for medullary sublineage divergence. *PLoS Genet.* **7**, e1002348.

**Ohnemus, S., Kanzler, B., Jerome-Majewska, L. A., Papaioannou, V. E., Boehm, T. and Mallo, M.** (2002). Aortic arch and pharyngeal phenotype in the absence of BMP-dependent neural crest in the mouse. *Mech. Dev.* **119**, 127-135.

**Ohuchi, H., Hori, Y., Yamasaki, M., Harada, H., Sekine, K., Kato, S. and Itoh, N.** (2000). FGF10 acts as a major ligand for FGF receptor 2 IIIb in mouse multi-organ development. *Biochem. Biophys. Res. Commun.* **277**, 643-649.

**Park, E. J., Sun, X., Nichol, P., Saijoh, Y., Martin, J. F. and Moon, A. M.** (2008). System for tamoxifen-inducible expression of cre-recombinase from the Foxa2 locus in mice. *Dev. Dyn.* **237**, 447-453.

**Patel, S. R., Gordon, J., Mahbub, F., Blackburn, C. C. and Manley, N. R.** (2006). Bmp4 and Noggin expression during early thymus and parathyroid organogenesis. *Gene Expr. Patterns* **6**, 794-799.

**Revest, J.-M., Suniara, R. K., Kerr, K., Owen, J. J. T. and Dickson, C.** (2001). Development of the thymus requires signaling through the fibroblast growth factor receptor r2-iiib. *J. Immunol.* **167**, 1954-1961.

**Senoo, M., Pinto, F., Crum, C. P. and McKeon, F.** (2007). p63 Is essential for the proliferative potential of stem cells in stratified epithelia. *Cell* **129**, 523-536.

**Soza-Ried, C., Bleul, C. C., Schorpp, M. and Boehm, T.** (2008). Maintenance of thymic epithelial phenotype requires extrinsic signals in mouse and zebrafish. *J. Immunol.* **181**, 5272-5277.

**Su, D.-M., Ellis, S., Napier, A., Lee, K. and Manley, N. R.** (2001). Hoxa3 and pax1 regulate epithelial cell death and proliferation during thymus and parathyroid organogenesis. *Dev. Biol.* **236**, 316-329.

**Su, D.-M., Navarre, S., Oh, W.-J., Condie, B. G. and Manley, N. R.** (2003). A domain of Foxn1 required for crosstalk-dependent thymic epithelial cell differentiation. *Nat. Immunol.* **4**, 1128-1135.

**Wang, J., Nagy, A., Larsson, J., Dudas, M., Sucov, H. M. and Kaartinen, V.** (2006). Defective ALK5 signaling in the neural crest leads to increased postmigratory neural crest cell apoptosis and severe outflow tract defects. *BMC Dev. Biol.* **6**, 51.

**Wei, Q. and Condie, B. G.** (2011). A focused in situ hybridization screen identifies candidate transcriptional regulators of thymic epithelial cell development and function. *PLoS ONE* **6**, e26795.

**Zamisch, M., Moore-Scott, B., Su, D.-M., Lucas, P. J., Manley, N. and Richie, E. R.** (2005). Ontogeny and regulation of IL-7-expressing thymic epithelial cells. *J. Immunol.* **174**, 60-67.